

# Fast Geometric Embedding for Node Influence Maximization

Alexander Kolpakov\* and Igor Rivin†

\*University of Austin, Email: akolpakov@uaustin.org

†Temple University, Email: rivin@temple.edu

**Abstract**—Computing classical centrality measures such as betweenness and closeness is computationally expensive on large-scale graphs. In this work, we introduce an efficient force layout algorithm that embeds a graph into a low-dimensional space, where the radial distance from the origin serves as a proxy for various centrality measures. We evaluate our method on multiple graph families and demonstrate strong correlations with degree, PageRank, and paths-based centralities. As an application, it turns out that the proposed embedding allows to find high-influence nodes in a network, and provides a fast and scalable alternative to the standard greedy algorithm.

## I. INTRODUCTION

Graph centrality measures provide crucial insights into network structure and influence. However, the computation of combinatorial measures such as betweenness or closeness is often infeasible for graphs with a large amount of vertices  $n$ , as it often grows as  $O(n^2)$  in practice, and cannot be parallelized. In contrast, spectral and force-directed methods are inherently parallelizable, and thus offer scalable alternatives.

This paper proposes a force layout algorithm that leverages a Laplacian-based initialization followed by iterative force updates to produce an embedding where the radial distance reflects node importance. We further explore potential applications of this embedding, in particular to finding high-importance communities, and compare our embedding to the baseline greedy algorithm using random cascades.

## II. METHOD DESCRIPTION

### A. Spectral Initialization

We begin with a Laplacian embedding of the graph to capture its global structure. This initialization provides a low-dimensional starting point that preserves important spectral properties.

### B. Force-Directed Refinement

Starting from the spectral layout  $P^{(0)} \in \mathbb{R}^{d \times n}$ , we perform  $T$  iterations of combined spring and intersection–repulsion updates.

1) *Spring Forces*. For each edge  $e = (i, j) \in E$ , let

$$\Delta_{ij} = p_i - p_j, \quad d_{ij} = \|\Delta_{ij}\| + \varepsilon,$$

where  $\varepsilon > 0$  is a small constant (say, on the order of  $\varepsilon = 10^{-6}$ ). The elastic Hooke’s force exerted on  $i$  by  $j$  is

$$F_{ij}^{\text{spring}} = -k_{\text{attr}} (d_{ij} - L_{\min}) \frac{\Delta_{ij}}{d_{ij}}.$$

Summing over all neighbors gives

$$F_i^{\text{spring}} = \sum_{j:(i,j) \in E} F_{ij}^{\text{spring}}.$$

2) *Intersection Detection*. To discourage crossing edges, we test every pair  $e = (u, v)$  and  $f = (w, x)$  for intersection via the oriented–area predicates

$$\text{orient}(a, b, c) = (b_x - a_x)(c_y - a_y) - (b_y - a_y)(c_x - a_x).$$

Edges cross if and only if

$$\text{orient}(u, v, w) \cdot \text{orient}(u, v, x) < 0,$$

and

$$\text{orient}(w, x, u) \cdot \text{orient}(w, x, v) < 0.$$

3) *Repulsion at Crossings*. For each intersecting pair  $(e, f)$ , compute their common midpoint

$$m_{e,f} = \frac{p_u + p_v + p_w + p_x}{4}.$$

Then each endpoint  $i \in \{u, v, w, x\}$  is subject to a repulsive force

$$F_{i,e,f}^{\text{intersect}} = k_{\text{inter}} \frac{p_i - m_{e,f}}{\|p_i - m_{e,f}\|^2 + \varepsilon}.$$

Summing over all crossing pairs yields

$$F_i^{\text{intersect}} = \sum_{(e,f) \text{ crossing}} F_{i,e,f}^{\text{intersect}}.$$

4) *Position Update and Normalization*. We combine the two force components and then re-center and rescale:

$$P = P^{(t)} + F^{\text{spring}} + F^{\text{intersect}},$$

$$P^{(t+1)} = \frac{P - \mu}{\sigma + \varepsilon},$$

where

$$\mu = \frac{1}{n} \sum_{i=1}^n p_i, \quad \sigma = \sqrt{\frac{1}{n} \sum_{i=1}^n \|p_i - \mu\|^2},$$

which prevents uncontrolled drift and stretching.

### III. THEORETICAL ANALYSIS

Below we present some theoretical analysis of our algorithm, and of why it may work for some classes of graphs. It seems that a detail analysis is only possible under some assumptions imposing the graph structure, while we would rather opt for a more general and possibly more heuristic argument. Nevertheless, it seems that the algorithm shows consistently strong results on both synthetic and real world datasets of various kinds, thus showing its practical tenability.

#### A. Fixed point existence

Given the formulas above, we have a smooth transition map  $\mathcal{T} = \mathcal{N} \circ \mathcal{F}$ , where

$$\mathcal{F}(P) = P + F^{\text{spring}} + F^{\text{intersect}}$$

is the force flow, and

$$\mathcal{N}(P) = \frac{1}{\sigma}(P - \mu)$$

is the normalization map.

Let us note that setting

$$\|P\|^2 = \frac{1}{n} \sum_{i=1}^n \|p_i\|^2$$

together with the fact that

$$\mu(P) = 0, \sigma(P) = 1,$$

readily implies that

$$\|\mathcal{N}(P)\| = 1.$$

The latter means  $\|\mathcal{F}(P)\| = 1$ , which yields  $\|p_i\| \leq \sqrt{n}$ , for any  $i = 1, \dots, n$ , and for every  $P = P^{(t)}$ , except  $t = 0$ . Thus, the map  $\mathcal{F}$  maps a closed ball containing the points  $p_i$  into itself. By Brouwer's fixed point theorem, there exists a fixed point  $P \in \mathbb{R}^{d \times n}$  such that  $\mathcal{F}(P) = P$ . At this point, the force layout comes to an equilibrium.

#### B. Energy and Lagrangian

The energy functional associated to the layout is

$$\begin{aligned} \mathcal{E}(P) &= \frac{k_{\text{attr}}}{2} \sum_{(i,j) \in E} (\|p_i - p_j\| - L_{\min})^2 \\ &+ \sum_{(e,f) \in \mathcal{I}(i)} \frac{k_{\text{inter}}}{\|p_i - m_{e,f}\|^2}, \end{aligned}$$

where

$$\mathcal{I}(i) = \{(e, f) \in E \times E \mid e = (i, j), f = (u, v), \\ e \text{ and } f \text{ intersect.}\}$$

The normalization map means imposing the constraints

$$\sum_{i=1}^n p_i = 0, \quad \frac{1}{n} \sum_{i=1}^n \|p_i\|^2 = 1.$$

Thus, we end up minimizing the Lagrangian

$$\mathcal{L}(P, \lambda, \mu) = \mathcal{E}(P) - \lambda \cdot \sum_{i=1}^n p_i - \mu \left( \sum_{i=1}^n \|p_i\|^2 - n \right),$$

where  $\lambda \in \mathbb{R}^d$  is a vector Lagrange multiplier for centering, and  $\alpha \in \mathbb{R}$  is the multiplier for the variance constraint.

Now, we get the following gradient of  $\mathcal{L}(P, \lambda, \mu)$  with respect to a node embedding  $p_i$ :

$$\nabla_{p_i} \mathcal{L}(P, \lambda, \mu) = \nabla_{p_i} \mathcal{E}(P) - \lambda - 2\mu p_i = 0.$$

Let  $\mathbf{r}_i = \frac{p_i}{\|p_i\|}$  be the unit vector pointing at  $p_i$ , i.e. the radial direction towards  $p_i$ . Let us note that  $\mathcal{E}(P)$  is translation-invariant, and thus

$$\nabla_q(P + q) = \sum_{i=1}^n \nabla_{p_i}(P) = 0$$

which, given the above expression for  $\nabla_{p_i} \mathcal{E}(P)$ , implies

$$0 = \sum_{i=1}^n \nabla_{p_i} \mathcal{E}(P) = \lambda n + 2\alpha \sum_{i=1}^n p_i = \lambda n + 2\alpha 0 = \lambda n,$$

Then we get

$$\nabla_{p_i} \mathcal{E}(P) = 2\alpha \|p_i\| \mathbf{r}_i,$$

and thus minimizing the energy largely results in the radial decrement

$$p_i^{(t+1)} = p_i^{(t)} - \eta \nabla_{p_i} \mathcal{E}(P),$$

where  $\eta > 0$  is the learning rate of the gradient descent.

Thus, after sufficiently many steps, we may assume

$$p_i = p_j + c_{ij} d_{ij} \mathbf{r}_i + k_{ij} \mathbf{r}_i^\perp,$$

$$p_i = m_{e,f} + c_{e,f} \|p_i\| \mathbf{r}_i + l_{ij} \mathbf{r}_i^\perp,$$

for any  $(e, f) \in \mathcal{I}(i)$ , and positive  $c_{ij}$  and  $c_{e,f}$ .

#### C. Equilibrium equations

For each node  $i$ , the equilibrium state of the force layout means that

$$F_i^{\text{spring}} + F_i^{\text{intersect}} = 0,$$

which transforms into

$$\begin{aligned} k_{\text{attr}} \sum_{j: (i,j) \in E} (d_{ij} - L_{\min}) \frac{p_i - p_j}{d_{ij}} \\ = k_{\text{inter}} \sum_{(e,f) \in \mathcal{I}(i)} \frac{p_i - m_{e,f}}{\|p_i - m_{e,f}\|^2}. \end{aligned}$$

Putting  $\delta_i = \frac{1}{\deg(i)} \sum_j c_{ij} (d_{ij} - L_{\min})$ , we get

$$\begin{aligned} k_{\text{attr}} \deg(i) \delta_i \mathbf{r}_i &= k_{\text{inter}} \sum_{(e,f) \in \mathcal{I}(i)} \frac{p_i}{c_{e,f} \|p_i\|^2} \\ k_{\text{attr}} \deg(i) \delta_i \mathbf{r}_i &= \frac{k_{\text{inter}}}{\|p_i\|} \sum_{(e,f) \in \mathcal{I}(i)} \frac{1}{c_{e,f}} \mathbf{r}_i. \end{aligned}$$

The latter implies the following equality for the coefficients

$$\|p_i\| = \frac{k_{\text{inter}}}{k_{\text{attr}} \deg(i) \delta_i} \sum_{(e,f) \in \mathcal{I}(i)} \frac{1}{c_{e,f}}$$

Now, if the sum above on the right satisfies

$$\text{int}(i) = \sum_{(e,f) \in \mathcal{I}(i)} \frac{1}{c_{e,f}} = \alpha \deg(i)^{1+\beta}$$

we obtain

$$\|p_i\| = \gamma \deg(i)^\beta,$$

which would immediately imply that the Spearman correlation of  $\|p_i\|$  and the degree centrality  $\deg(i)$  is positive.

The assumption on  $\text{int}(i)$  is reasonable. Let us assume that the edges in the neighborhood of  $p_i$  have the same intersection probability  $\rho$ , and that the degree does not vary too much, i.e. for all  $j$  such that  $(i, j) \in E$ , we have  $\deg(j) = O(\deg(i))$ , then the number of edge intersections in the neighborhood of  $p_i$  is about  $O(\rho \deg(i)^2)$ .

The sum over the edge intersections  $\text{int}(i)$  in the neighborhood of a given node embedding  $p_i$  may as well be expressible via the vertex betweenness  $\text{btw}(i)$ , as shortest paths along the edges *not* incident to  $i$  may result in intersecting the edges incident to  $i$  in the embedding (since we need to have an “overpass” atop the neighborhood of  $p_i$ ).

This assumption, however, does not need to hold, as vertices of relatively low degree may have high betweenness (e.g. vertices of bridge edges). Other centrality measures may also be proportional to  $\text{int}(i)$ , though in general none of them has to. Nevertheless, many graphs demonstrate correlation of degree centrality and other centrality measures [Val+08].

#### IV. ACHIEVING EFFICIENCY

In order to achieve computational efficiency, we reduce the computation of intersection forces  $F^{\text{intersect}}$  to an analogous computation on the  $k$  nearest neighbor ( $kNN$ ) graph of midpoints of intersecting edges. This avoids overwhelming computational load if the number of intersections is much larger than  $O(E)$ .

The  $kNN$  graph can be efficiently computed, especially if  $k$  is not very large, and a theoretical algorithm would take about  $O(E^{1+\tau})$ , steps, with  $\tau \in (0, 1)$  [CFS09]. Also, approximate  $kNN$  methods are known to be very efficient in practice [DCL11]. However, subsampling the midpoints together with GPU/TPU acceleration [Bra+18] makes the runtime much shorter. After that, the repulsion forces  $F^{\text{intersect}}$  are computed within  $O(kE)$  steps.

The attraction forces  $F^{\text{spring}}$  are naturally provided by the graph connectivity structure, and take  $O(E)$  steps to compute.

#### V. NUMERICAL EXPERIMENTS

We evaluated our method on several synthetic graph families, including Erdős-Renyi [ER59], Watts-Strogatz [WS98], power law cluster [HK02], and balanced tree graphs, as well as real world datasets. For each graph, we computed standard centrality measures: degree, betweenness [Fre79; Bra01], eigenvector [Bon72], PageRank [BP98], closeness [FRM79; Fre79], and node load [GKK01], and compared them with the radial distances from our embedding using Spearman correlation. We also provide its confidence interval with confidence level  $\gamma = 0.95$ , obtained by bootstrapping.

##### A. Experimental Setup

The force layout is computed using a JAX-based implementation [KR25] with a specified number of iterations, attraction

and repulsion parameters, and a user-defined embedding dimension. Correlation coefficients are calculated between the radial distance and each centrality measure. In practice, our algorithm shows strong correlations in hub-dominated networks, while preserving rank order in hierarchical structures.

##### B. Synthetic Datasets

Tables I–II summarize the correlations for Erdős-Renyi graphs [ER59], Tables III–IV are for Watts-Strogatz graphs [WS98], and Tables V–VI for power law cluster graphs [HK02]. These results demonstrate that in small-world and scale-free networks, the radial distance strongly approximates global centrality in the sense of the ordering of nodes by centrality.

Here we use Spearman’s  $\rho$  correlation instead of Pearson’s correlation as the relationship between radial ordering and centrality is not necessarily linear (as the force layout is highly non-linear), and because what matters most is the ordering, not the actual distance or centrality values.

In all cases we can observe that embeddings in dimension 2 already demonstrate good correlation between the radial distance and centrality measures. However, as the embedding dimension growth up to 4, all correlations become stronger. There could be a slight increase in correlations after dimension 4; however, it is on the order of magnitude smaller than between dimension 2 and 4. More experimental data is available on GitHub [KR25].

On the other hand, being a planar graph the balanced ternary tree shows best correlations between the radial distance in the embedding and vertex centralities in dimension 2, see Table VII. These correlations visibly deteriorate in higher dimensions, as shown in Table VIII.

Centrality Measure	$\rho$	95% CI	$p$
Degree	0.829	[0.803, 0.854]	$< 10^{-6}$
Betweenness	0.845	[0.817, 0.867]	$< 10^{-6}$
Eigenvector	0.806	[0.778, 0.833]	$< 10^{-6}$
PageRank	0.835	[0.807, 0.859]	$< 10^{-6}$
Closeness	0.830	[0.802, 0.855]	$< 10^{-6}$
Node Load	0.845	[0.818, 0.866]	$< 10^{-6}$

TABLE I: Spearman correlations of centrality measures with the radial distance in graph embeddings for Erdős – Renyi graphs. Embedding dimension 2.

Centrality Measure	$\rho$	95% CI	$p$
Degree	0.963	[0.956, 0.968]	$< 10^{-6}$
Betweenness	0.966	[0.959, 0.971]	$< 10^{-6}$
Eigenvector	0.948	[0.939, 0.955]	$< 10^{-6}$
PageRank	0.965	[0.959, 0.970]	$< 10^{-6}$
Closeness	0.963	[0.956, 0.968]	$< 10^{-6}$
Node Load	0.966	[0.960, 0.970]	$< 10^{-6}$

TABLE II: Spearman correlations of centrality measures with the radial distance in graph embeddings for Erdős – Renyi graphs. Embedding dimension 4.

We also present some visual “before-and-after” images of the initial Laplacian embeddings of graphs in dimensions 2 and 3 (“before”) and their finalized force layout embeddings (“after”). Each embedding has the vertices color-labeled according

Centrality Measure	$\rho$	95% CI	$p$
Degree	0.896	[0.877, 0.912]	$< 10^{-6}$
Betweenness	0.748	[0.718, 0.776]	$< 10^{-6}$
Eigenvector	0.646	[0.605, 0.682]	$< 10^{-6}$
PageRank	0.897	[0.878, 0.912]	$< 10^{-6}$
Closeness	0.594	[0.549, 0.633]	$< 10^{-6}$
Node Load	0.743	[0.711, 0.771]	$< 10^{-6}$

TABLE III: Spearman correlations of centrality measures with the radial distance in graph embeddings for Watts–Strogatz graphs. Embedding dimension 2.

Centrality Measure	$\rho$	95% CI	$p$
Degree	0.956	[0.948, 0.962]	$< 10^{-6}$
Betweenness	0.810	[0.784, 0.831]	$< 10^{-6}$
Eigenvector	0.711	[0.676, 0.742]	$< 10^{-6}$
PageRank	0.947	[0.937, 0.955]	$< 10^{-6}$
Closeness	0.656	[0.621, 0.691]	$< 10^{-6}$
Node Load	0.804	[0.779, 0.826]	$< 10^{-6}$

TABLE IV: Spearman correlations of centrality measures with the radial distance in graph embeddings for Watts–Strogatz graphs. Embedding dimension 4.

Centrality Measure	$\rho$	95% CI	$p$
Degree	0.783	[0.750, 0.814]	$< 10^{-6}$
Betweenness	0.635	[0.590, 0.678]	$< 10^{-6}$
Eigenvector	0.411	[0.353, 0.463]	$< 10^{-6}$
PageRank	0.805	[0.773, 0.832]	$< 10^{-6}$
Closeness	0.352	[0.297, 0.407]	$< 10^{-6}$
Node Load	0.644	[0.598, 0.692]	$< 10^{-6}$

TABLE V: Spearman correlations of centrality measures with the radial distance in graph embeddings for power law cluster graphs. Embedding dimension 2.

Centrality Measure	$\rho$	95% CI	$p$
Degree	0.866	[0.841, 0.888]	$< 10^{-6}$
Betweenness	0.733	[0.696, 0.766]	$< 10^{-6}$
Eigenvector	0.561	[0.516, 0.600]	$< 10^{-6}$
PageRank	0.869	[0.845, 0.892]	$< 10^{-6}$
Closeness	0.500	[0.451, 0.546]	$< 10^{-6}$
Node Load	0.738	[0.700, 0.770]	$< 10^{-6}$

TABLE VI: Spearman correlations of centrality measures with the radial distance in graph embeddings for power law cluster graphs. Embedding dimension 4.

Centrality Measure	$\rho$	95% CI	$p$
Degree	0.816	[0.810, 0.822]	$< 10^{-6}$
Betweenness	0.772	[0.769, 0.774]	$< 10^{-6}$
Eigenvector	0.670	[0.660, 0.680]	$< 10^{-6}$
PageRank	0.830	[0.823, 0.837]	$< 10^{-6}$
Closeness	0.772	[0.770, 0.775]	$< 10^{-6}$
Node Load	0.772	[0.769, 0.775]	$< 10^{-6}$

TABLE VII: Spearman correlations of centrality measures with the radial distance in graph embeddings for balanced ternary trees. Embedding dimension 2.

to the vertex degree normalize to the interval from 0 (minimum degree) to 1 (maximum degree). One can observe that how high-centrality vertices are moved towards the periphery in the case of a random Erdős–Rényi (Figure 1), a grid graph (Figure 2), and a balanced ternary tree (Figure 3).

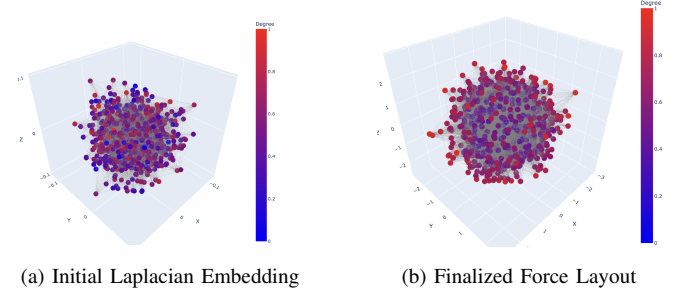


Fig. 1: The initial embedding and the final layout. Vertex degrees (normalized to  $[0, 1]$ ) are shown in color: blue = lower degree, red = higher degree. Here an Erdős–Rényi graph is used with  $n = 1000$  vertices, and edge probability  $p = 0.025$ .

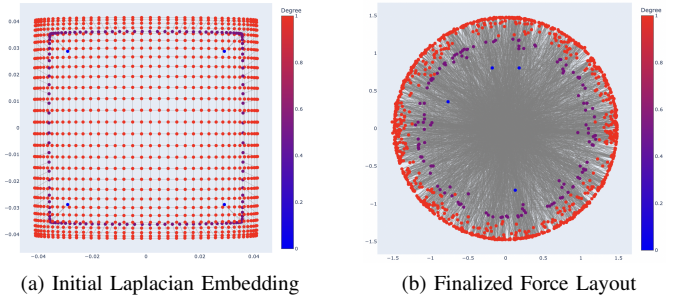


Fig. 2: The initial embedding and the final layout. Vertex degrees (normalized to  $[0, 1]$ ) are shown in color: blue = lower degree, red = higher degree. Here the grid graph with  $30 \times 40$  squares is used.

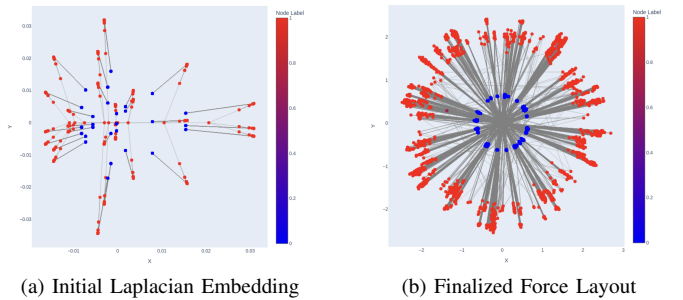


Fig. 3: The initial embedding and the final layout. Vertex degrees (normalized to  $[0, 1]$ ) are shown in color: blue = lower degree, red = higher degree. Here the balanced ternary tree with 8 levels is used. A few vertices and edges appear to coincide in the initial embedding.

Centrality Measure	$\rho$	95% CI	$p$
Degree	0.479	[0.462, 0.497]	$< 10^{-6}$
Betweenness	0.463	[0.446, 0.480]	$< 10^{-6}$
Eigenvector	0.428	[0.412, 0.446]	$< 10^{-6}$
PageRank	0.477	[0.460, 0.495]	$< 10^{-6}$
Closeness	0.463	[0.446, 0.480]	$< 10^{-6}$
Node Load	0.463	[0.446, 0.480]	$< 10^{-6}$

TABLE VIII: Spearman correlations of centrality measures with the radial distance in graph embeddings for balanced ternary trees. Embedding dimension 4.

### C. Real World Datasets

We use several dataset from SNAP [LK14] in order to test the algorithm’s effectiveness on large scale real world data:

- “General Relativity and Quantum Cosmology collaboration network” [LKF07b; LKF07a] in Table IX;
- “Social Circles: Facebook” [LM12; ML12] in Table X;
- “Wikipedia vote network” [LHK08; LHK10], with 74% of the vertices (and 55% of all edges) being subsampled to reduce the complexity of computation for combinatorial centrality measures, in Table XI. Degree, eigenvector and PageRank centralities can be computed for the entire dataset, and the resulting correlations are shown in Table XII.

For disconnected graphs we use the largest connected component for benchmarking. For very large graphs, since computing combinatorial centralities may not be feasible, we use subsampling. We also compare three embedding dimensions for our benchmarks,  $d = 3, 4$ , and 6, and record the best one. More benchmarks are available on GitHub [KR25].

Centrality Measure	$\rho$	95% CI	$p$
Degree	0.834	[0.817, 0.850]	$< 10^{-5}$
Betweenness	0.770	[0.757, 0.785]	$< 10^{-5}$
Eigenvector	0.370	[0.344, 0.395]	$< 10^{-5}$
PageRank	0.839	[0.826, 0.853]	$< 10^{-5}$
Closeness	0.450	[0.422, 0.477]	$< 10^{-5}$
Node Load	0.770	[0.755, 0.784]	$< 10^{-5}$

TABLE IX: Spearman correlations of centrality measures with the radial distance in a graph embedding for the SNAP “General Relativity and Quantum Cosmology collaboration network” dataset [LKF07b]. Embedding dimension 6.

Centrality Measure	$\rho$	95% CI	$p$
Degree	0.864	[0.851, 0.877]	$< 10^{-5}$
Betweenness	0.721	[0.704, 0.740]	$< 10^{-5}$
Eigenvector	0.537	[0.513, 0.560]	$< 10^{-5}$
PageRank	0.746	[0.730, 0.763]	$< 10^{-5}$
Closeness	0.592	[0.571, 0.610]	$< 10^{-5}$
Node Load	0.718	[0.698, 0.736]	$< 10^{-5}$

TABLE X: Spearman correlations of centrality measures with the radial distance in a graph embedding for the SNAP “Social circles: Facebook” dataset [LM12]. Embedding dimension 4.

## VI. NODE INFLUENCE OPTIMIZATION

Influence optimization is a central task in such domains as viral marketing, mathematical epidemiology, and social network analysis. While traditional greedy algorithms iteratively

Centrality Measure	$\rho$	95% CI	$p$
Degree	0.955	[0.950, 0.959]	$< 10^{-5}$
Betweenness	0.934	[0.928, 0.939]	$< 10^{-5}$
Eigenvector	0.852	[0.840, 0.863]	$< 10^{-5}$
PageRank	0.952	[0.947, 0.956]	$< 10^{-5}$
Closeness	0.839	[0.827, 0.850]	$< 10^{-5}$
Node Load	0.933	[0.928, 0.938]	$< 10^{-5}$

TABLE XI: Spearman correlations of centrality measures with the radial distance in a graph embedding for the SNAP “Wikipedia vote network” dataset [LHK08]. Embedding dimension 3. We subsampled 5250 vertices to reduce combinatorial complexity.

Centrality Measure	$\rho$	95% CI	$p$
Degree	0.964	[0.961, 0.967]	$< 10^{-5}$
Eigenvector	0.871	[0.863, 0.879]	$< 10^{-5}$
PageRank	0.958	[0.954, 0.962]	$< 10^{-5}$

TABLE XII: Spearman correlations of centrality measures with the radial distance in a graph embedding for the SNAP “Wikipedia vote network” dataset [LHK08]. Complete dataset with 7115 vertices and 103689 edges. Embedding dimension 3.

select nodes based on their highest marginal gains in influence, this approach is often offset by its substantial computational cost.

### A. Synthetic Dataset

In our experiments, random Erdős–Renyi graphs were used with  $n = 128$  nodes and edge probability  $p = 0.05$ . We used the Independent Cascades (IC) method with adjacent node activation probability  $p_{ic} = 0.1$  and  $k = 10$  seed vertices. The IC algorithm was realized by using NDlib library [Ros+16]. The benchmark was repeated 50 time to collect a statistical sample. The outcomes of using the graph embedding as opposed to the classical greedy seed selection are given in Table XIII for comparison.

Method	Influence	Iterations	Time (s)
Embedding	$24.6 \pm 6.9$	200	$0.26 \pm 0.48$
Greedy	$23.7 \pm 5.1$	247200	$15.97 \pm 0.08$

TABLE XIII: Influence spread, number of NDlib simulation iterations, and runtime for embedding-based vs. greedy method. Synthetic dataset: a random Erdős–Renyi graph on 128 nodes with edge probability  $p = 0.05$ .

### B. Real World Dataset

As a real world dataset, we use the “General Relativity and Quantum Cosmology collaboration network” dataset [LKF07b]. Its largest connected component has 4158 nodes and 13428 edges, which is within reasonable bounds to run greedy search for maximum influence subsets (while the graph embedding would work efficiently for much larger datasets). The benchmarking results are given in Table XIV.

Method	Spread	Iterations	Time (s)
Embedding	$23.9 \pm 6.0$	200	$0.19 \pm 0.01$
Greedy	$22.9 \pm 5.7$	247,200	$15.95 \pm 0.07$

TABLE XIV: Influence spread, number of NDlib simulation iterations, and runtime for embedding-based vs. greedy method. Real world dataset: “General Relativity and Quantum Cosmology collaboration network” [LKF07b].

## VII. OTHER EMBEDDINGS

In this section we check if other graph embeddings produce radial distance correlated with centrality measures. We produced embeddings in dimension  $d = 2$  by the following widely used methods: Laplacian eigenmap, UMAP [MHM18; Dev25], TriMAP [AW19], PaCMAP [Wan+21; Dev20]. As inputs, we used random Erdős–Rényi graphs on 1000 vertices with vertex probability 0.05. There was no statistically significant Spearman correlation observed in any of the considered cases, see Tables XV, XVI, XVII, and XVIII. A visual inspection confirms the findings, as evidenced in Figure 4.

Centrality Measure	$\rho$	95% CI	$p$
Degree	−0.018	[−0.079, 0.047]	0.563
Betweenness	−0.026	[−0.078, 0.033]	0.408
Eigenvector	−0.025	[−0.084, 0.037]	0.428
PageRank	−0.016	[−0.078, 0.047]	0.605
Closeness	−0.050	[−0.109, 0.023]	0.111
Node Load	−0.027	[−0.090, 0.035]	0.400

TABLE XV: Laplacian eigenmaps and centrality measures *do not* exhibit statistically significant Spearman correlation.

Centrality Measure	$\rho$	95% CI	$p$
Degree	−0.009	[−0.069, 0.046]	0.765
Betweenness	−0.020	[−0.080, 0.042]	0.532
Eigenvector	−0.013	[−0.080, 0.047]	0.679
PageRank	−0.008	[−0.077, 0.054]	0.790
Closeness	−0.038	[−0.101, 0.024]	0.235
Node Load	−0.020	[−0.083, 0.041]	0.519

TABLE XVI: UMAP embedding and centrality measures *do not* exhibit statistically significant Spearman correlation.

Centrality Measure	$\rho$	95% CI	$p$
Degree	−0.008	[−0.072, 0.057]	0.811
Betweenness	−0.017	[−0.075, 0.049]	0.587
Eigenvector	−0.012	[−0.077, 0.051]	0.694
PageRank	−0.006	[−0.072, 0.054]	0.844
Closeness	−0.038	[−0.098, 0.022]	0.231
Node Load	−0.018	[−0.079, 0.045]	0.574

TABLE XVII: TriMAP embedding and centrality measures *do not* exhibit statistically significant Spearman correlation.

Centrality Measure	$\rho$	95% CI	$p$
Degree	−0.023	[−0.081, 0.038]	0.462
Betweenness	−0.029	[−0.096, 0.039]	0.363
Eigenvector	−0.031	[−0.089, 0.037]	0.333
PageRank	−0.021	[−0.079, 0.041]	0.507
Closeness	−0.051	[−0.101, 0.009]	0.104
Node Load	−0.029	[−0.089, 0.035]	0.355

TABLE XVIII: PaCMAP embedding and centrality measures *do not* exhibit statistically significant Spearman correlation.

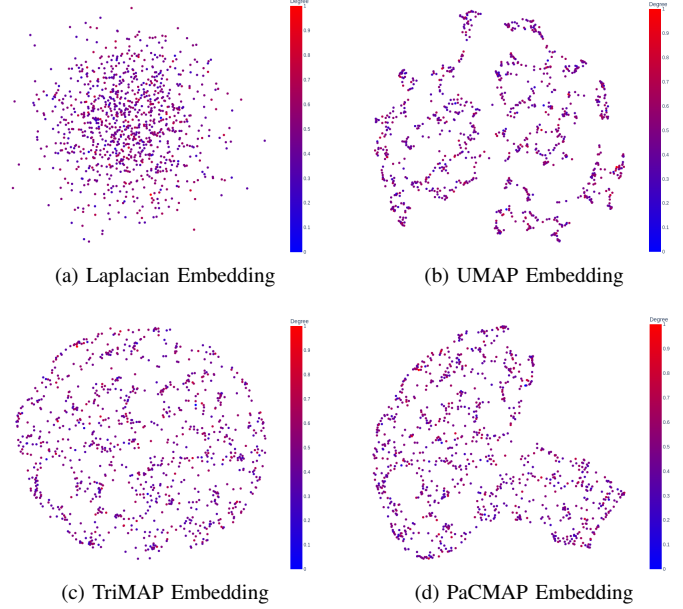


Fig. 4: Graph layout produced by the Laplacian eigenmap, UMAP, TriMAP, and PaCMAP. The input is a random Erdős–Rényi graph with 1000 vertices and edge probability 0.05. Vertex degrees (normalized to  $[0, 1]$ ) are shown in color: blue = lower degree, red = higher degree.

## VIII. DISCUSSION

We produce a new graph embedding method that provides a proxy for node centrality in a wide variety of graph classes, as is evidenced by our experiences on both synthetic and real world datasets. The method’s convergence and properties also have a mathematical backing, although some assumptions should be made.

Other graph embedding methods, of similar kin, do not exhibit strong statistical correlation between the radial distance to the embedded nodes and their importance, even in relatively common and simple classes of graphs such as random Erdős–Rényi graphs.

### CODE AND DATA AVAILABILITY

The code used in the present paper is publicly available on GitHub [KR25]. All data is either generated by this code (synthetic datasets), or available from SNAP [LK14] (real world datasets).

### ACKNOWLEDGMENTS

This work is supported by the Google Cloud Research Award number GCP19980904.

### REFERENCES

- [ER59] Paul Erdős and Alfréd Rényi. “On Random Graphs I”. In: *Publicationes Mathematicae* 6 (1959), pp. 290–297.

- [Bon72] Phillip Bonacich. “Factoring and weighting approaches to status scores and clique identification”. In: *Journal of Mathematical Sociology* 2.1 (1972), pp. 113–120. DOI: 10.1080/0022250X.1972.9989806.
- [Fre79] Linton C. Freeman. *Centrality in Social Networks: Conceptual Clarification*. Vol. 1. 3. Elsevier, 1979, pp. 215–239.
- [FRM79] Linton C. Freeman, Douglas Roeder, and Robert R. Mulholland. “Centrality in social networks: II. Experimental results”. In: *Social Networks* 2 (1979), pp. 119–141.
- [BP98] Sergey Brin and Lawrence Page. “The anatomy of a large-scale hypertextual Web search engine”. In: *Computer Networks and ISDN Systems* 30.1-7 (1998), pp. 107–117.
- [WS98] Duncan J. Watts and Steven H. Strogatz. “Collective dynamics of ‘small-world’ networks”. In: *Nature* 393.6684 (1998), pp. 440–442. DOI: 10.1038/30918.
- [Bra01] Ulrik Brandes. “A faster algorithm for betweenness centrality”. In: *Journal of Mathematical Sociology* 25.2 (2001), pp. 163–177.
- [GKK01] K.-I. Goh, B. Kahng, and D. Kim. “Universal behavior of load distribution in scale-free networks”. In: *Physical Review Letters* 87.27 (2001), p. 278701. DOI: 10.1103/PhysRevLett.87.278701.
- [HK02] Petter Holme and Beom Jun Kim. “Growing scale-free networks with tunable clustering”. In: *Physical Review E* 65.2 (2002), p. 026107. DOI: 10.1103/PhysRevE.65.026107.
- [LKF07a] Jure Leskovec, Jon Kleinberg, and Christos Faloutsos. “Graph Evolution: Densification and Shrinking Diameters”. In: *ACM Transactions on Knowledge Discovery from Data (TKDD)* 1.1 (2007), p. 2. DOI: 10.1145/1217299.1217301.
- [LKF07b] Jure Leskovec, Jon Kleinberg, and Christos Faloutsos. *Graph of coauthorships in the e-print arXiv General Relativity and Quantum Cosmology category*. <http://snap.stanford.edu/data/ca-GrQc.html>. From: J. Leskovec, J. Kleinberg and C. Faloutsos. Graph Evolution: Densification and Shrinking Diameters. ACM TKDD, 1(1), 2007. Accessed: 2025-06-01. 2007.
- [LHK08] Jure Leskovec, Daniel Huttenlocher, and Jon Kleinberg. *Wikipedia Vote Network*. <http://snap.stanford.edu/data/wiki-Vote.html>. Accessed: 2025-06-01. 2008.
- [Val+08] Thomas W. Valente et al. “How correlated are network centrality measures?” In: *Connections* 28.1 (2008), pp. 16–26.
- [CFS09] Jie Chen, Haw-ren Fang, and Yousef Saad. “Fast Approximate kNN Graph Construction for High Dimensional Data via Recursive Lanczos Bisection”. In: *Journal of Machine Learning Research* 10 (2009), pp. 1989–2012. URL: <https://jmlr.org/papers/volume10/chen09b/chen09b.pdf>.
- [LHK10] Jure Leskovec, Daniel Huttenlocher, and Jon Kleinberg. “Signed Networks in Social Media”. In: *Proceedings of the SIGCHI Conference on Human Factors in Computing Systems*. ACM, 2010, pp. 1361–1370.
- [DCL11] Wei Dong, Moses Charikar, and Kai Li. “Efficient k-nearest neighbor graph construction for generic similarity measures”. In: *Proceedings of the 20th International Conference on World Wide Web (WWW ’11)*. New York, NY, USA: Association for Computing Machinery, 2011, pp. 577–586. DOI: 10.1145/1963405.1963487. URL: <https://dl.acm.org/doi/10.1145/1963405.1963487>.
- [LM12] Jure Leskovec and Julian J. McAuley. *Facebook Social Circles Network Dataset*. <http://snap.stanford.edu/data/egonets-Facebook.html>. From: J. McAuley and J. Leskovec, Learning to Discover Social Circles in Ego Networks, NIPS 2012. Accessed: 2025-06-01. 2012.
- [ML12] Julian McAuley and Jure Leskovec. “Learning to Discover Social Circles in Ego Networks”. In: *Advances in Neural Information Processing Systems 25 (NIPS 2012)*. Accessed: 2025-06-01. Curran Associates, Inc., 2012, pp. 539–547. URL: <https://papers.nips.cc/paper/4532-learning-to-discover-social-circles-in-ego-networks>.
- [LK14] Jure Leskovec and Andrej Krevl. *SNAP Datasets: Stanford Large Network Dataset Collection*. <http://snap.stanford.edu/data>. Accessed: 2025-06-01. 2014.
- [Ros+16] Giulio Rossetti et al. *NDlib: A Python Library to Model and Analyze Diffusion Processes on Complex Networks*. <https://github.com/GiulioRossetti/ndlib>. Accessed: 2025-06-01. 2016.
- [Bra+18] James Bradbury et al. *JAX: composable transformations of Python+NumPy programs*. Version 0.3.13. 2018. URL: <http://github.com/google/jax>.
- [MHM18] Leland McInnes, John Healy, and James Melville. “UMAP: Uniform Manifold Approximation and Projection”. In: *Journal of Open Source Software* 3.29 (2018), p. 861. DOI: 10.21105/joss.00861. URL: <https://doi.org/10.21105/joss.00861>.
- [AW19] Ehsan Amid and Manfred K Warmuth. “TriMap: large-scale dimensionality reduction using triplets”. In: *arXiv preprint arXiv:1910.00204* (2019).
- [Dev20] PaCMAP Developers. *PaCMAP: Pairwise Controlled Manifold Approximation*. <https://github.com/YingfanWang/PaCMAP>. Accessed: 2025-06-07. 2020.
- [Wan+21] Yingfan Wang et al. “Understanding how dimension reduction tools work: an empirical approach to deciphering t-SNE, UMAP, TriMAP, and PaCMAP for data visualization”. In: *JMLR* 22.201 (2021), pp. 1–73.

- [Dev25] UMAP Developers. *Uniform Manifold Approximation and Projection (UMAP)*. <https://github.com/lmcinnes/umap/>. 2025.
- [KR25] Alexander Kolpakov and Igor Rivin. *GraphEm: Graph Embedding for efficient centrality approximation*. <https://github.com/sashakolpakov/graphem>. 2025.